PHYSICAL REVIEW LETTERS

VOLUME 62 | 20 FEBRUARY 1989 | NUMBER 8

Precise Determination of the Cooper-Pair Mass

J. Tate,[a] B. Cabrera, S. B. Felch,[b] and J. T. Anderson[c]

Physics Department, Stanford University, Stanford, California 94305

(Received 5 December 1988)

The ratio h/m' of Panck's constant to the observable Cooper-pair mass ($\sim 2m_e$) is determined directly using a rotating superconducting ring by measuring the London moment flux $(2m'c/e^*)\omega S$, where S is the area bounded by the ring, in units of the flux quantum (hc/e^*). The flux in the ring is zero for a set of rotation frequencies which are equally spaced by $\Delta\nu$, and $h/m' = 2S\Delta\nu$. We have measured $\Delta\nu$ and S with a precision of 5 ppm and an accuracy of 21 ppm. Our result for niobium, $(m'/2m_e)_{\rm Nb} = 1.000\,084(21)$, disagrees with theoretical predictions of 0.999 992.

PACS numbers: 06.20.Jr, 71.10.+x, 74.90.+n

A rotating superconductor has a uniform magnetic field throughout its interior given by $B_L = -(2m^*c/e^*)\omega$, as first predicted by London[1] and verified experimentally to a few percent.[2] Higher-precision measurements of the mass parameter are possible by determining the London flux through a rotating ring in terms of an area S and the flux quantum $\phi_0 = hc/e^*$ as first reported by Zimmerman and Mercereau,[3] later by Parker and Simmonds,[4] and most recently by ourselves.[5] Unlike the flux quantum ϕ_0, shown theoretically and experimentally to contain no relativistic corrections ($e^* \equiv -2|e|$), the mass appearing in the London magnetic field is expected to differ from the free-electron mass m_e.[6-10] The Cooper-pair mass parameter m^* is defined as the proportionality constant between the velocity $\mathbf{v}$ and momentum $m^*\mathbf{v} = (h/2\pi)\nabla\varphi - (e^*/c)\mathbf{A}$, where φ is the phase of the macroscopic order parameter and $\mathbf{A}$ is the magnetic vector potential. The deviations from $2m_e$ arise from two sources. First, the mass of the composite Cooper pair contains a large kinetic-energy term for electrons near the Fermi surface such that m^* is greater than $2m_e$ by about 180 ppm for niobium (on this scale the binding energy of a Cooper pair is negligible). We call this mass m^* the intrinsic Cooper mass. Second, there is a contribution to the magnetic vector potential $\mathbf{A}$ within the superconductor which arises from the motion of the internal electrostatic potential in the laboratory frame. Since this contribution to $\mathbf{A}$ cannot be observed from outside the metal, it is convenient to define an observable mass m' such that $m^*\mathbf{v} + (e^*/c)\mathbf{A} = m'\mathbf{v} + (e^*/c)\mathbf{A}_{\rm obs}$, where now $\mathbf{A}_{\rm obs}$ contains only contributions from currents which can be measured from outside the superconductor. We find $\mathbf{A} = \mathbf{A}_{\rm obs} + (\mathbf{v}/c)\langle\Phi\rangle$, where $\langle\Phi\rangle$ is an averaged value of the electrostatic potential in the lattice.[8,10] This second correction is slightly greater than the first in magnitude and of opposite sign so that it is predicted that m' is less than $2m_e$ by ~ 8 ppm for niobium. In this paper, we report on an experimental determination of m' of sufficient accuracy to probe the relativistic regime for the first time.

To analyze our experiment, we consider flux quantization and the London moment in a rotating superconducting ring within the framework of the Ginzburg-Landau current equation, suitably modified to include the effects of rotation. We may use nonrelativistic equations because the rotation velocity $\mathbf{v} = \boldsymbol{\omega} \times \mathbf{r}$ is at most 1 m/s. In this limit, the relativistic corrections are included in the parameter m', and the effect of rotation is kinematically equivalent to the application of a uniform magnetic field (or an additional vector potential) so that

$$(4\pi\lambda^2/c)\,\mathbf{j} = (hc/2\pi e^*)\nabla\varphi - \mathbf{A}_{\rm obs} - (m'c/e^*)\,\boldsymbol{\omega}\times\mathbf{r}\,, \qquad (1)$$

where λ is the London penetration depth. Integrating

Eq. (1) around the ring for a closed path Γ entirely within the superconductor and requiring that the order parameter be single valued, we obtain

$$(4\pi\lambda^2/c)\int_\Gamma \mathbf{j}\cdot d\mathbf{l} = n(hc/e^*) - \phi_{\rm obs} - (2m'c/e^*)\boldsymbol{\omega}\cdot\mathbf{S}, \quad (2)$$

where S is the area bounded by Γ and n is an integer. This equation relates the observed flux $\phi_{\rm obs}$ through the ring to its rotation rate, $\omega = 2\pi\nu$, and describes a family of parallel straight lines, one for each n. Figure 1 shows our experimental data for $\phi_{\rm obs}$ vs ν. There exists a frequency ν_n for each n such that the flux $\phi_{\rm obs}$ and $\mathbf{j}$ are zero together. We define the flux null spacing by $\Delta\nu \equiv \nu_n - \nu_{n-1}$ and subtract equations for n and $n-1$ to obtain

$$h/2\pi m' = 2S\Delta\nu, \quad (3)$$

the primary relation used to analyze our experiment.

The superconducting ring in our experiment is a thin-film band of niobium, 20 μm wide and 40 nm thick, deposited on the equator of a fused-quartz rotor. The position and dimensions of the ring ensure that its area differs from the cross-sectional area of the rotor by less than 2 ppm. The area bounded by the ring is determined from absolute diameter measurements together with a roundness verification. We used an interferometric technique[11] to measure two perpendicular diameters at the operating temperature of the experiment. The average diameter at 6 K is 5.075835(22) cm with the uncertainty primarily due to the optical aperture, location of fringe centers, and phase changes on reflection. We measured the roundness at room temperature with a Talyrond,[12] and found that the out-of-roundness contributes less than 2 ppm to the uncertainty in the area.

Figure 2 shows the apparatus used to measure the flux null spacing.[5] The fused-quartz rotor, which is slightly more than a hemisphere and approximately 5 cm in diameter, is levitated and spun about its symmetry axis in a helium-gas bearing at 6 K. The tolerances of the bearing constrain the area vector and spin axis of Eq. (2) to be coincident to better than a milliradian. We use rotation frequencies up to 5 Hz in either direction that are stabilized to 1 mHz with feedback control. A frosted pattern on the rotor top flat modulates the intensity of reflected light and this signal is used for determining the average frequency to seven-digit accuracy. For the magnetic-flux readout, the current in the ring couples inductively to the external pickup loop of a SQUID magnetometer which is located in a groove in the rotor housing and remains stationary as the ring rotates. The flux measurement is gated by a frequency counter so that each point in Fig. 1 represents the speed and flux averaged over an integer number of rotations. Between measurements, different quantum states n in Eq. (2) are accessed because a section of the Nb ring is driven normal by a heat pulse from a 789-nm pulsed laser diode via an optical fiber. The most likely flux state is the one with the least current, and higher current states are accessed with decreasing probability such that the distribution is Gaussian.[13] The entire apparatus is encased in a double-walled vacuum jacket surrounded by a superconducting lead shield,[14] which maintains the ambient magnetic field at 5×10^{-8} G.

In early runs, we found that the dominant systematic shift in the flux null spacing was caused by electrostatic charging of the rotor surface. The presence of this charge introduces an additional rotation-rate-dependent term into Eq. (2), which results in a correction to m' in

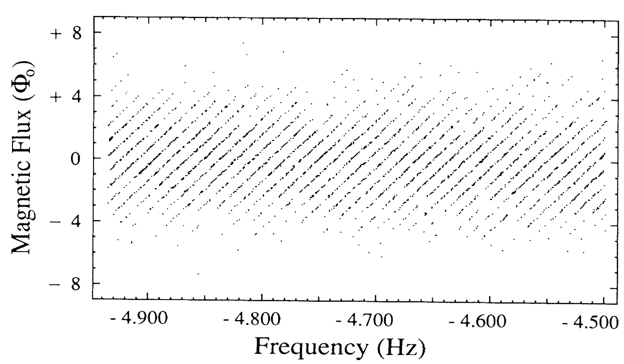

FIG. 1. SQUID output as a function of rotation rate over a 440-mHz interval.

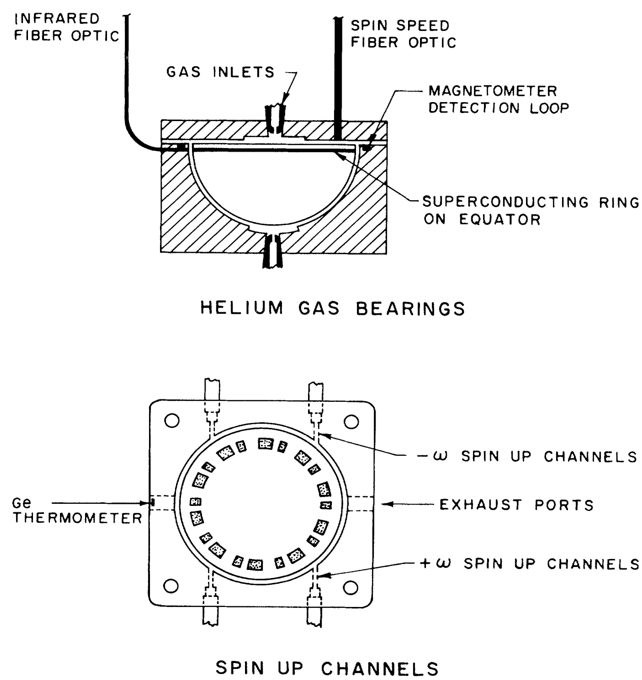

FIG. 2. Schematic of rotating superconductor apparatus made of fused quartz.

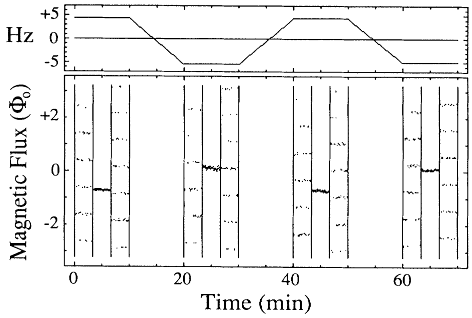

FIG. 3. Data acquisition scheme to simultaneously measure m' and rotor charge.

Eq. (3). We measured the surface charge by monitoring the change of flux with rotation rate above and below T_c, expressing the ratio as $\delta \equiv (\partial\phi/\partial\omega)_{\rm normal}/(\partial\phi/\partial\omega)_{\rm supercond}$. We also calculated the effect of a charge distribution on $\Delta\nu$, and found

$$\Delta\nu(\delta) = \Delta\nu(0)(1-\epsilon\delta), \qquad (4)$$

where ϵ is a constant which depends on the charge distribution. For a uniform distribution $\epsilon = 0.70$, and for a general surface or volume distribution it deviates from this value by less than a few percent, as long as the charge distribution varies slowly within ~ 1 mm of the niobium line.[5] Attempts to eliminate the charge with ionizing α sources and grounded surfaces succeeded in reducing its size and produced a distribution of δ about zero, allowing a good fit with Eq. (4).

The data-taking procedure[15] outlined in Fig. 3 exploited the linear relation in Eq. (4) to extract the flux spacing at zero charge. With the ring superconducting, we set the rotor at a constant speed and took seventy flux per frequency data pairs, then rapidly changed the frequency by ~ 2 or ~ 8 Hz and took seventy more pairs. Between each pair, the ring was driven normal at the same spot by the laser heat pulse. These data fall into well-defined flux states, allowing the number of unrecorded flux nulls between the two frequencies to be determined by the method of exact fractions. The intercept ν_n on the $\phi = 0$ axis was obtained for each point, using the previously determined London moment slope. We obtained $\Delta\nu$ from the slope of the least-squares straight-line fit to the points (ν_n, n). The corresponding value for δ was found from the slope of the straight-line fit to the pairs of flux per frequency points taken when the ring was normal.

Using Eq. (3) to obtain m' from $\Delta\nu$, we plot $m'/2m_e$ against δ and obtain Fig. 4 which contains 630 points (206 with $\sim$2-Hz interval and 424 with $\sim$8-Hz interval, of which 27 were reported earlier[5]). The linear relation $m'(\delta)/2m_e = m'(0)/2m_e(1+\epsilon\delta)$ predicted by Eq. (4) is verified and we obtain an experimental value of $\epsilon = 0.695(7)$ in agreement with the value predicted from calculations based on the geometry. Trapping of a vortex in the niobium ring can cause large and nonstatistical deviations in the results, so the best-fit slope to our data is obtained by discarding any points that lie more than 2.5 standard deviations from the least-squares straight line of all data. Then, in an iterative process known as Chauvenet's criterion[16] we recompute the least-squares straight line and standard deviation from the remaining data and discard data points until none lie outside of 2.5 standard deviations (15% of the data points were discarded). We find that the Cooper-pair mass in the absence of a rotor charge is $(m'/2m_e)_{\rm Nb} = 1.000084(5)$, determined by the intercept of the best-fit line with the $\delta = 0$ axis. The inset in Fig. 4 shows the distribution of all points translated to $\delta = 0$ with slope $\epsilon = 0.695$, and is consistent with the scatter expected from the SQUID $1/f$ noise spectrum.

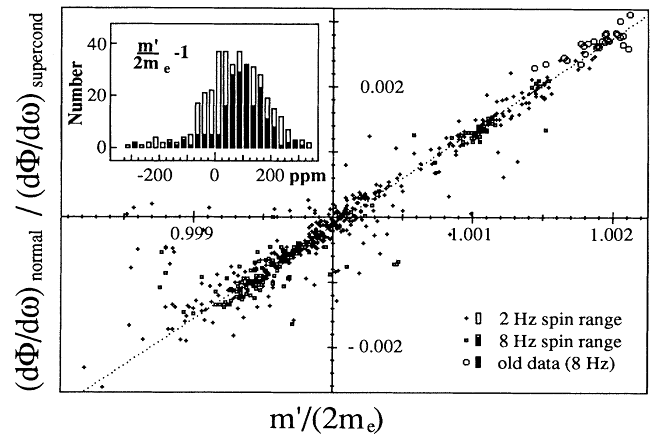

FIG. 4. The measured value of m' as a function of rotor charge. Inset: Superimposed distributions of m' values about the least-squares line ($\epsilon = 0.695$) for $\sim$2-Hz and $\sim$8-Hz intervals.

The error quoted above is statistical, but systematic errors also exist and are summarized in Table I. The magnetic susceptibility of fused quartz produces a volume magnetization as the rotor spins (Barnett moment), which is mathematically equivalent to a surface-current distribution. It is accounted for by the fitting procedure described above, as is any systematic motion of the rotor-housing assembly in the magnetic gradient of the shield. Drifts in the SQUID output result from changes in the helium bath temperature and have the same effect whether the ring is normal or superconducting ($\epsilon = 1$). It produces a slight symmetric broadening in the data distribution along the line in Fig. 4, but will shift the intercept for an asymmetric range of δ. The vertical motion of the rotor in the housing produces changes in the SQUID output, due to modulation of the mutual inductance between the ring and the pickup loop in nonuniform magnetic fields which are generated by a current in the pickup loop itself. We reduced this motion sensitivity by nulling the current trapped in the pickup

TABLE I. Error budget for determination of m' in ppm.

Flux null spacing determination	
Statistical fit for rotation-dependent moments ($\epsilon=0.70$)	± 5
Nonuniform charge distribution ($\epsilon \neq 0.70$)	± 5
SQUID drift ($\epsilon=1$)	± 2
Motion of rotor position within housing	± 18
Frequency counter	± 0.1
Area determination and fundamental constants	
$S=20.235\,057(179)$ cm^{2} [a]	± 8.9
$h=6.626\,075\,5(40)\times 10^{-34}$ J s [b]	± 0.60
$m_e=9.109\,389\,7(54)\times 10^{-31}$ kg [b]	± 0.59
Cooper-pair mass	
$(m'/2m_e)_{\mathrm{Nb}}=1.000\,084(21)$	± 21

[a]From Ref. 11.
[b]From Ref. 17.

loop. However, the possible errors from this effect dominate our systematic error budget and would be reduced by directly monitoring the position of the rotor in the housing with an improved optical system. The runs reported here were taken over several years with many changes in the apparatus which would affect these systematics. Remarkably, the data from all of these runs, as well as our earlier data from four years ago[5] (see "old data" in Fig. 4), consistently fall on a universal straight line, indicating that remaining systematics are small.

In conclusion, we have obtained the first data for the Cooper-pair mass in the relativistic region, and our result disagrees with theory. In fact, the result is almost halfway between the predicted values for the observable mass m' and the intrinsic mass m^* and ~ 5 standard deviations from each. In the next phase of the experimental work, we intend to perform a differential measurement comparing two superconductors with high precision which will avoid many of the systematic effects seen here. As for the theory, all published work to data has been based on mean-field analysis of the macroscopic fields. We believe that an approach based on a relativistic microscopic many-body theory may be needed, to account properly for all lowest-order relativistic contributions.[18]

We acknowledge the important early contributions to this experiment by W. M. Fairbank, G. Hess for the design of the quartz gas bearing, D. Davidson for its construction, and G. Siddall for the room-temperature area determination. We also thank W. A. Little and C. W. F. Everitt for many helpful discussions. This research has been funded in part by NSF Grants No. 80-26007 and No. 84-05384 and by a Precision Measurement Grant from NBS.

(a)Present address: Physik Department E10, Technische Universität München, D-8046 Garching, Federal Republic of Germany.

(b)Present address: Varian Associates, Palo Alto, CA 94303.

(c)Present address: Hewlett Packard Laboratories, Palo Alto, CA 94303.

1F. H. London, *Superfluids* (Wiley, New York, 1950), Vol. 1.

2A. F. Hildebrandt, Phys. Rev. Lett. **12**, 190 (1964).

3J. E. Zimmerman and J. E. Mercereau, Phys. Rev. Lett. **12**, 887 (1965).

4W. H. Parker and M. B. Simmonds, U.S. National Bureau of Standards Special Publication No. 343 (U.S. GPO, Washington, DC, 1970).

5S. B. Felch, J. Tate, B. Cabrera, and J. T. Anderson, Phys. Rev. B **31**, 7006 (1985).

6P. W. Anderson (quoting B. D. Josephson), in *Progress in Low Temperature Physics,* edited by C. J. Gorter (North-Holland, Amsterdam, 1967), Vol. 5.

7R. M. Brady, J. Low Temp. Phys. **49**, 1 (1982).

8B. Cabrera, H. Gutfreund, and W. A. Little, Phys. Rev. B **25**, 6644 (1982).

9J. Anandan, Phys. Lett. **105A**, 280 (1984).

10B. Cabrera and M. E. Peskin, Phys. Rev. B (to be published).

11J. Tate, D. H. McIntyre, and B. Cabrera (to be published).

12B. Cabrera and G. J. Siddall, Precis. Eng. **3**, 125 (1981).

13J. Tate, B. Cabrera, and S. B. Felch, in *Proceedings of the Seventeenth International Conference on Low Temperature Physics,* edited by U. Eckern, A. Schmidt, W. Weber, and H. Wühl (North-Holland, Amsterdam, 1984), p. 1179.

14B. Cabrera and F. van Kann, Acta Astron. **5**, 125 (1978).

15J. Tate, Ph.D. thesis, Stanford University, 1987 (unpublished); J. Tate, B. Cabrera, S. B. Felch, and J. T. Anderson (to be published).

16H. D. Young, *Statistical Treatment of Experimental Data* (McGraw-Hill, New York, 1962), pp. 78–80.

17E. R. Cohen and B. N. Taylor, J. Res. Natl. Bur. Stand. **92**, 85 (1987).

18G. Baym, University of Illinois Report No. P/8709/183 (to be published).